Title
Magnetic resonance imaging in the evaluation of ligament injuries

Journal
Skeletal Radiology, 28(2)

ISSN
0364-2348

Authors
Farooki, Shella
Seeger, LL

Publication Date
1999-02-01

DOI
10.1007/s002560050476

Peer reviewed

Skeletal Radiol (1999) 28:61–74

REVIEW ARTICLE

Shella Farooki
Leanne L. Seeger

Magnetic resonance imaging in the evaluation of ligament injuries

Received: 4 August 1998
Revision requested: 1 October 1998
Revision received: 23 October 1998
Accepted: 29 October 1998

S. Farooki, M.D. · L.L. Seeger, M.D. (✉)
UCLA School of Medicine,
Department of Radiological Sciences,
200 Medical Plaza, Suite 165–57,
Los Angeles, CA 90095–6952, USA

Abstract Magnetic resonance imaging has had a dramatic effect on the means by which we diagnose ligament injuries. Tears resulting from either acute trauma or overuse can be detected noninvasively, directing appropriate therapy be it conservative or surgical. For the elite athlete, earlier diagnosis leads to earlier intervention, or alternatively, a normal MRI examination can result in an earlier return to play. While MRI is accepted for the diagnosis of certain injuries such as complete tears of the cruciate ligaments of the knee, other injuries, such as partial cruciate ligament tears or tears of the intercarpal ligaments of the wrist, remain controversial.

Key words Ligament · Ligament injury · MRI · Soft tissue injury · Soft tissue trauma

Introduction

Magnetic resonance imaging (MRI) has revolutionized diagnostic imaging of ligamentous injuries. In the past, arthrography was used to diagnose ligamentous tears. Complete ligamentous tears may be evident on clinical examination or through inference by malalignment of bony structures. The diagnosis of a ligament tear can be compromised in the setting of an acute injury by the presence of soft tissue swelling, joint effusion, and pain. Partial thickness tears, often resulting from chronic overuse, could often only be diagnosed with exploratory surgery or clinical observation until complete ligament rupture occurred. The ability to obtain high-resolution images of ligaments has thus resulted in earlier intervention, be it conservative or surgical. In cases where surgery is undertaken, less extensive procedures may be possible as the surgeon has preoperative access to information regarding the exact location and size of the tear.

Wrist

The preferred means to image intrinsic derangements of the wrist remains controversial. Traditionally, triple-compartment wrist arthrography has been the gold standard, with positive contrast injected into the radiocarpal joint (RCJ), distal radioulnar joint (DRUJ), and midcarpal joint (MCJ). This allows identification of tears of the scapholunate (SL) ligament and lunotriquetral (LT) ligament (Fig. 1) as well as tears of the triangular fibrocartilage complex (TFCC). In more recent years, there has been a great interest in MRI for evaluation of the wrist (Fig. 2). Dedicated surface coils have been developed to optimize signal-to-noise ratio and contrast resolution with small field-of-view images. Important in decision-making regarding imaging modality is the fact the arthrography is only minimally invasive, and the cost is substantially less than that of MRI [1].

Arguments favoring MRI over arthrography include its noninvasive nature and the ability to directly image not only the intercarpal ligaments and TFCC, but also extrinsic ligaments, tendons, nerves and [2, 3]. The decision to use arthrography versus MRI should include evaluation of the accuracy of each as compared with the surgical findings. Early studies indicated that MRI was inferior to arthrography in detecting SL ligament tears [1]. A more recent study of asymptomatic volunteers and arthrographically normal wrists indicated that the LT ligament can be consistently seen with MRI, but the appearance is

Fig. 1 Lunotriquetral tear with conventional arthrography, posteroanterior projection. Following injection of the radiocarpal joint, contrast is seen between the lunate and triquetrum (*arrow*), indicating a tear of the ligament

Fig. 2 Lunotriquetral ligament tear with MRI. Coronal gradient echo MR image (38/15) showing focal high signal intensity in the expected region of the ligament (*arrow*). Courtesy of Tom Learch, M.D.

Fig. 3 Gamekeeper's thumb. Posteroanterior radiograph of the thumb showing an avulsion fracture (*arrow*) at the base of the proximal phalanx

Fig. 4 Ulnar collateral ligament tear of the elbow. Coronal fast inversion recovery MR image (4000/30) showing complete disruption of the ligament (*arrow*)

Fig. 5 Ulnar collateral ligament avulsion. Anteroposterior radiograph showing an avulsion fracture of the sublime tubercle of the ulna (*arrow*), a finding that is diagnostic of this injury

highly variable [4]. Another study concluded that the three portions of the SL ligament can be differentiated with three-dimensional gradient-recalled-echo imaging [5]. The MR appearance of the extrinsic wrist ligaments has also been described [6–9], but the clinical application of imaging these ligaments is limited.

A positioning device has been used to track carpal motion with MRI [10,11]. Although considered a "kinematic" study, this device acquires multiple static images that are played on a cine loop. For a simpler, truly dynamic study of carpal instability, the wrist can be taken through active or passive range of motion under fluoroscopic control, either videotaping the examination or taking pertinent spot films. This method also allows correlation of audible or palpable clicks with specific wrist motion and alignment anomalies.

Patient positioning for wrist MRI can be challenging. Ideally, the wrist should be as close to the isocenter of the magnet as possible, requiring positioning with the shoulder in full extension (over the head). Regardless of whether this is accomplished with the patient supine or prone, the position is uncomfortable for most individuals, resulting in motion artifact that greatly degrades the images. If the scans are acquired with the arm at the side, the signal-to-noise ratio can be compromised by the substantial off-center shift.

MR arthrography of the wrist has been described. In the evaluation of SL ligament perforations, MR arthrography has been shown to be slightly more accurate than conventional MRI with arthroscopy as the standard, but conventional MRI and MR arthrography were equally accurate for detection of LT tears [12]. Thus, there does not appear to be sufficient significance to justify intra-articular injection on a routine basis. In addition, injection prior to MRI negates the noninvasive nature of the MR study, and injection of iodinated contrast (a conventional

arthrogram) rather than gadolinium identifies intercarpal ligament perforations, negating the need for the MR study.

Common to both arthrography and MRI is the fact that degenerative perforations of the interosseous ligaments are common in people older than 35 years of age [13–15]. Manaster et al. [16] have found that arthrographic findings correlate well with ulnar-sided wrist pain, but are less sensitive for radial-sided pain. More recently, Metz et al. [17] found no association with the side of pain and the defect. As one could expect similar results with conventional arthrography and MRI, the clinical significance of a tear with either modality in the middle-aged and older population is in question.

Hand

Gamekeeper's thumb refers to an acute or chronic injury of the ulnar collateral ligament (UCL), which extends from the ulnar aspect of the first metacarpal to the proximal phalanx. The UCL is a major stabilizing structure of the first metacarpophalangeal joint. Gamekeeper's thumb was first described by Campbell et al. [18] in Scottish gamekeepers, whose occupation resulted in stress and subsequent stretching of the UCL. Currently, UCL injuries are most often seen in skiers who suddenly hyperextend or hyperabduct the thumb when using ski poles.

The diagnosis of complete UCL tear or avulsion can be made clinically and with plain radiography (Fig. 3) and stress radiography or arthrography. When the UCL is ruptured distally, the proximal torn end may fold upon itself, and the adductor pollicis aponeurosis can become trapped between the ruptured end of the ligament and its bony attachment site, thereby preventing healing. This complication is known as the Stener lesion [19], and surgical repair is generally indicated. There is controversy as to whether surgical repair is indicated for patients with clinical findings of a complete UCL tear without an osseous abnormality or intra-articular displacement of the aponeurosis. Some surgeons argue that the UCL is a capsular ligament, and nonoperative treatment is adequate for nondisplaced tears [20, 21]. The utility of imaging must thus be gauged according to whether or not the results will alter patient management.

Radiographs may demonstrate an avulsed bone fragment which suggests the diagnosis of UCL tear or avulsion, but radiographs cannot distinguish between displaced and nondisplaced tears. MRI has been used to evaluate the presence and extent of UCL injuries [22–24], with specificities ranging from 67% [22] to 100% [24]. A recent study in cadavers comparing conventional arthrography, both low-field-strength and high-field-strength MRI as well as low- and high-field MR arthrography showed that high-field MR arthrography was overall superior to the other methods [25].

Elbow

MRI applications in the evaluation of the elbow joint are limited compared with those in other appendicular joints. Technical obstacles include the complexity of designing a surface coil to accommodate the geometry of the elbow in partial flexion (a common position of injury on locking) and techniques that allow imaging of the elbow joint at the patient's side, removed from the scanner isocenter.

MRI is successful in characterizing occult fractures, osteochondral lesions, and tendinous and ligamentous trauma of the elbow [26–28]. One of the more common applications is for investigating the integrity of the medial (ulnar, UCL) and lateral (radial, RCL) collateral ligaments. Although there have been no large-scale studies to date, there appears to be a good correlation between findings on MRI and at surgery for the diagnosis of complete tears of the collateral ligaments of the elbow [29, 30].

The UCL of the elbow consists of three bands [31]. The anterior band is the strongest and functionally most important. It extends from the medial epicondyle of the humerus to the medial aspect of the coronoid process in an area sometimes referred to as the sublime tubercle. The posterior band extends from the medial epicondyle of the humerus to the medial aspect of the olecranon. The weaker transverse or oblique band bridges the ulnar attachments of the anterior and posterior bands. MR images reveal the UCL to be a thin, low signal intensity band, distal to the medial epicondyle. Injuries of the UCL are common in throwing athletes [32].

The RCL is a single band. Its apex is attached to the lateral epicondyle of the humerus, and its base is attached to the upper margin of the annular ligament. RCL injuries are less common than injuries to the UCL, but may be seen in tennis players and golfers.

For imaging of the collateral ligaments, the elbow should be in full extension. The ligaments, which are actually focal thickenings of the joint capsule, are best displayed in a plane along the long axis of the elbow joint, thus requiring oblique coronal imaging. In a recent cadaveric study, posterior coronal oblique imaging at an angle of 20° with the elbow in extension showed the best delineation of the anterior band of the UCL. Another useful technique reported is coronal imaging aligned along the long axis of the humeral shaft with the elbow in 20°–30° of flexion [33].

Complete tears of the UCL of the elbow are displayed on MRI as discontinuity between the ligament and its bony attachment or disruption of the ligament itself [27, 34] (Fig. 4). Partial tears are usually at the humeral insertion site [34]. Ligamentous strain will be evident as increased signal in the surrounding soft tissues, often in conjunction with thickening of the ligament [26, 27]. In addition to tearing, the UCL may avulse off the sublime tubercle [35] (Fig. 5). Although this injury is evident on

plain radiographs as a small calcific density adjacent to the tubercle, the MRI appearance has been described.

MRI has been described in the preoperative diagnosis of posterolateral rotatory instability of the elbow, an entity which results from disruption of the ulnar band of the RCL [36]. In a recent series, findings of posterolateral rotatory instability included abnormal increased signal at the proximal attachment of the RCL, full-thickness proximal detachment, midsubstance discontinuity, and nonvisualization that suggested a chronic tear [37]. All these study patients had an intact anterior portion of the RCL and an intact UCL.

While conventional MRI has been shown to be sensitive for detection of full-thickness collateral ligament tears, partial-thickness tears may not be well displayed [38]. In this setting, MR arthrography has been promoted, especially for the investigation of partial-thickness undersurface tears in throwing athletes [30]. These individuals would likely be considered for more aggressive therapy than the nonathletic population.

Knee

MRI is unparalleled in the assessment of the ligamentous structures of the knee, including the anterior cruciate ligament (ACL), posterior cruciate ligament (PCL), medial or tibial collateral ligament (TCL), and the fibular collateral ligament (FCL). Additional ligamentous structures in and around the knee that have been addressed in the literature include the meniscofemoral and transverse geniculate ligaments. These latter structures are important to recognize as normal structures to avoid confusion with a meniscal tear

Anterior cruciate ligament

The ACL is an intracapsular, extrasynovial structure. Proximally, it is attached to the posteromedial aspect of the lateral femoral condyle. It extends in an anterior, inferior, and medial direction to insert on the intercondylar eminence, between the anterior attachments of the menisci. The average ACL is 11 mm wide and 31–38 mm long [39].

The ACL is composed of two functional fiber bundles that cannot be differentiated on gross examination or with MRI (Fig. 6). The longer anteromedial bundle tightens with knee flexion, and the shorter, thicker posterolateral bundle tightens with extension. In flexion, the anteromedial fibers twist or spiral over the posterolateral fibers. The ACL prevents anterior translation of the tibia and the resists posterior translation of the femur [39].

The high sensitivity of MRI for detecting acute, complete tears of the ACL is well established. Disruption of the midsubstance is most common, accounting for 75% of all tears [40]. Tears of the femoral fibers are seen in 20% of cases, and distal fiber tears are seen in 5%.

Complete ACL tears are diagnosed on MRI as discontinuity in the ligament, an abnormal course (Fig. 7), or fluid within the ligament on T2-weighted images. Hemarthrosis is commonly seen within 12 h of an ACL tear [41]. The sensitivity and specificity of MRI for detecting acute ACL tears is high, and is generally felt to be over 90% [42, 43]. While some authors advocate imaging in a plane orthogonal to the ACL [44], this is usually not necessary for diagnosis as routine sagittal images suffice.

Several secondary signs for ACL tear have been described, including anterior displacement of tibia (the anterior drawer sign), reduced ACL angle, bone contusion, a positive PCL line, reduced PCL angle, and posterior displacement of the lateral meniscus [45].

While acute complete ACL tears generally present no diagnostic challenge with MRI, partial-thickness tears can be more problematic [46, 47]. Partial-thickness tears may be seen on MRI as mild bowing of the ligament [46]. Most likely, low-grade partial ACL tears are usually not evident, and high-grade partial tears appear to be complete disruption (Fig. 8).

Chronic complete ACL tears can be diagnosed with MRI, but many of the signs seen in the acute stage (fluid or edema within the tendon, joint effusion, marrow edema) will be lacking. Instead, the course of the ligament within the joint must be followed. Often, the ligament cannot be visualized on sagittal or coronal images. This direct sign is diagnostic of an ACL tear. If the tear occurred in the more proximal fibers of the ligament, the distal limb may drift inferiorly and scar down to the PCL (Fig. 9). In this instance, the course of the ligament will be the only indication of a prior tear. On clinical examination, the Lachman test will be equivocal, with a perceivable end point but one that is looser than normal.

Far less commonly than tearing, the ligament may avulse a bony attachment. Femoral avulsions are extremely uncommon [48]. Tibial avulsions, classically described in children who have fallen off a bicycle, can be seen in the adult population [49] (Fig. 10).

ACL reconstruction is now commonly performed, especially for the younger, athletic population. This procedure has a high success rate for providing stability. Intra-articular reconstruction techniques include the central third of the patellar tendon/bone or Achilles tendon allograft or autograft, and semitendinosis or gracilis autograft. For a combined intra- and extra-articular procedure, the iliotibial band is transferred intra-articularly in a lateral over-the-top reconstruction. Extra-articular techniques have fallen out of favor. Synthetic materials used in the past for ACL reconstruction include carbon fiber, knitted Dacron, braided polypropylene, polytetrafluoroethylene and Gore-Tex. This type of reconstruction has been associated with graft attenuation, rupture, stretching and synovitis, and these materials have generally been replaced by

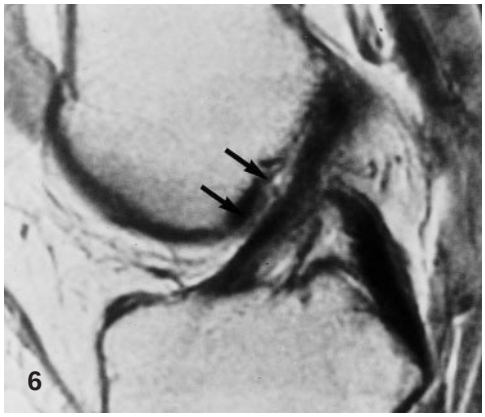

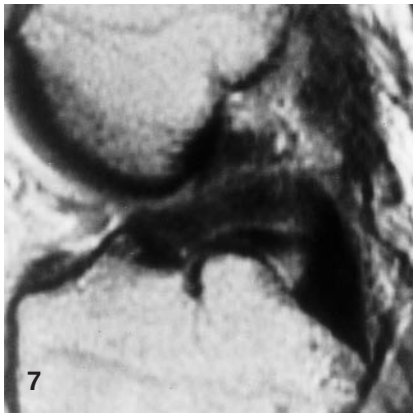

Fig. 6 Normal anterior cruciate ligament (ACL). Sagittal proton density MR image (SE 2000/20) showing the ligament extending between the tibial eminence and the lateral wall of the intercondylar notch. The ligament parallels the roof of the notch (*arrows*)

Fig. 7 Complete proximal ACL tear. Sagittal proton density MR image (SE 2000/15) showing the ligament has an abnormal horizontal course

Fig. 8 Partial ACL tear. Sagittal proton density MR image (SE 2200/15) showing an ill-defined ACL with inhomogeneous signal intensity. Although the ligament looks completely disrupted, a 75% tear was found at surgery

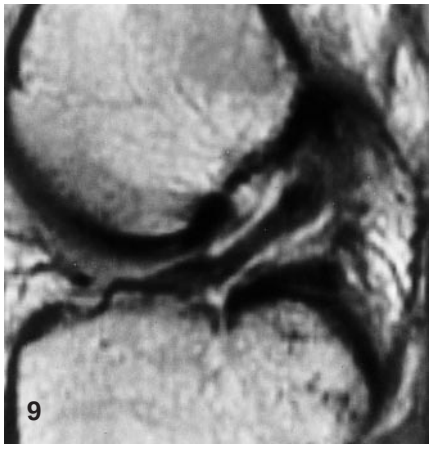

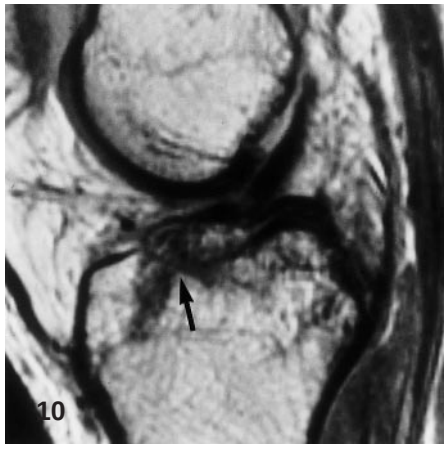

Fig. 9 Chronic ACL tear. Sagittal proton density MR image (SE 1800/15) showing a somewhat horizontal course of the ACL. The tear is through the proximal fibers. The ligament is completely surrounded by fluid, does not extend to the wall of the notch, and is probably scarred to the posterior cruciate ligament

Fig. 10 ACL avulsion. Sagittal proton density MR image (SE 1800/15) showing a fracture at the tibial attachment of the ACL (*arrow*). The fragment is slightly distracted, resulting in mild laxity of the ligament

auto- or allograft material. Regardless of the reconstruction technique used, the goal is to establish sufficient isometric tension to keep the distance between the tibial and femoral attachment points from changing more than 1–2 mm through 0° to 90° of flexion.

Postoperative assessment of ACL reconstruction is not limited by metallic artifact (Fig. 11). As with primary ACL tears, disruption of the graft is diagnostic of graft failure (Fig. 12). Torn graft may be seen as increased signal intensity and splaying of fibers with areas of fluid accumulation around separated fascicles [50]. Increased signal intensity without change in ligament morphology cannot be used as a primary criterion for diagnosing graft failure. Initially felt to be due to revascularization, this finding may be due to impingement on the graft by the intercondylar notch [48]. Likewise, an abnormal horizontal graft orientation is not a reliable sign of graft failure but may reflect poor tunnel placement [50]. The MR anterior drawer sign and buckling of the PCL may indicate abnormal laxity.

In addition to evaluation of graft integrity, the course of the graft should be noted [50–52]. The graft should be parallel to but not in contact with the notch, and there should be no angulation between the graft and the tibial tunnel. The notch should be adequate, and not impinge on the graft.

Posterior cruciate ligament

The PCL originates on the lateral aspect of the medial femoral condyle along the notch, crosses behind the ACL, and attaches to the posterior intercondylar fossa of the tibia. It is composed of anterolateral and posteromedial bands that tighten on flexion and extension, respectively. Viewed as a central stabilizer of the knee resisting posterior tibial displacement on the femur, the PCL protects against excessive varus or valgus angulation and resists internal rotation of the tibia on the femur. As the PCL is 2–3 times stronger than the ACL and has a larger cross-sectional area and a higher tensile strength [53, 54] there is a lower incidence of PCL rupture than ACL tear. For the same reasons, PCL avulsions are more

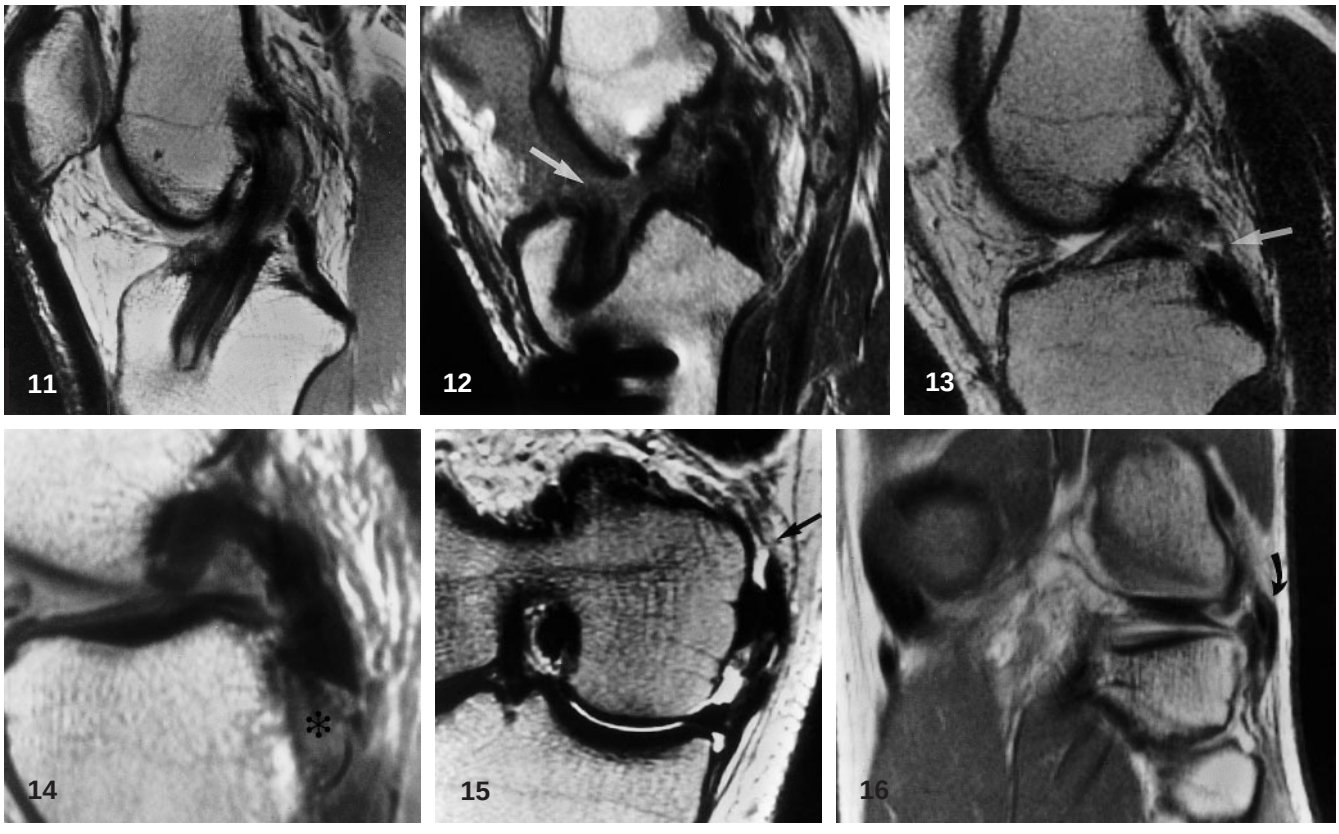

Fig. 11 Intact ACL graft. Sagittal proton density MR image (SE 1900/20) showing homogeneous signal throughout the ligament, a straight course into the tibial tunnel, and a smooth transition into the femoral tunnel

Fig. 12 Torn ACL graft. Sagittal proton density MR image (SE 2000/15) showing disruption of the graft (*arrow*)

Fig. 13 Torn posterior cruciate ligament (PCL). Sagittal T2-weighted MR image (SE 2066/70) showing high signal intensity fluid and disruption of the mid-substance of the PCL (*arrow*)

Fig. 14 PCL avulsion. Sagittal proton density MR image (SE 1800/20) showing separation of the distal PCL from the posterior tibia (*asterisk*)

Fig. 15 High-grade tibial collateral ligament tear. Coronal T2-weighted MR image (FSE 4000/105) showing complete disruption of the proximal fibers of the tibial collateral ligament (*arrow*)

Fig. 16 Fibular collateral ligament tear. Coronal proton density MR image (SE 2000/18) showing thickening of the ligament centrally (*arrow*), with attenuation of the fibers both proximally and distally

common that ACL avulsions. A posterior drawer sign indicates posterior tibial displacement and can be seen in up to 60% of PCL ruptures [55].

On sagittal images, the PCL is usually a uniform dark band. Any increase in signal on T1, T2, or T2* images within this normally low-signal ligament is generally abnormal (Fig. 13). With an acute tear, hemorrhage and edema cause less mass effect and distortion than in ACL tears. The PCL morphology may be normal, but abnormal signal will be present in the ligament. Partial tears may be more difficult to assess. Chronic tears with fibrous scarring demonstrate intermediate signal intensity on all pulse sequences.

PCL injuries are often associated with tears of the ACL, menisci, or collateral ligaments [56, 57]. Rupture can be caused by excessive rotation, hyperextension, dislocation, or direct trauma when the knee is flexed. Tears are most common in the midportion (68%), followed by proximal (19%) and distal tears (4%) [56].

Avulsions account for 7% of PCL injuries [57]. PCL avulsion at the tibial plateau may be associated with hemorrhage and high signal intensity in the distal ligament (Fig. 14). The avulsed bone fragment containing marrow may be seen attached to the ligament. If the fragment is nondisplaced or only minimally displaced, a PCL avulsion can be treated conservatively. If the fragment is distracted, surgical intervention is warranted.

Tibial collateral ligament

The tibial (medial) collateral ligament (TCL) can be considered to be composed of either two or three layers [58]. Most superficially, the deep fascia surrounding the sartorius and overlying gastrocnemius is found (layer 1). The superficial TCL (layer 2, the true TCL) lies beneath this

fascia. The deep TCL (layer 3), the medial capsular ligament, is the capsule of knee joint. Posteriorly, the superficial and deep TCL form the posterior oblique ligament. The TCL is separated from the underlying capsular ligament and the medial meniscus by a bursa that reduces friction during knee flexion. When the knee is extended, the TCL is taut and limits hyperextension. The TCL remains taut throughout flexion, where it provides primary valgus stability.

TCL injuries are usually associated with a valgus force applied to a flexed knee, and are graded according to severity [59]. Grade 1 TCL injuries are associated with mild to moderate pain but no instability. Grade 2 injuries are partial tears with mild functional instability. Grade 3 injuries are complete ruptures with gross instability. Complete TCL tears are often associated with ACL tears, meniscal tears, and tears of the medial and posterior capsule. The classic O'Donohue triad of ACL, TCL, and medial meniscal tear has recently been challenged. Several authors have found the combined ACL/TCL injury to be most often associated with tears of the lateral meniscus, not the medial [60, 61].

With MRI, coronal images best demonstrate the normal low signal intensity TCL and its attachments. Separation of deep and superficial layers can occasionally be seen on T2-weighted images. A thin band of intermediate signal, an intraligamentous bursa, may be seen between the anterior portion of the TCL and the deep or medial capsular ligament. This does not represent a pathologic separation, but increased signal above or below the level of the meniscus is pathologic where layers 2 and 3 fuse.

A grading system has been applied to TCL injuries with MRI [62]. In grade 1 injuries, edema and hemorrhage that parallels the TLC is seen. This may extend into the subcutaneous tissues. The TCL is usually of normal thickness and closely applied to underlying cortical bone. Grade 2 injuries demonstrate morphologic disruption and high signal intensity fluid in the TCL bursa. Varying degrees of edema and/or hemorrhage may be present superficial and deep to the TCL depending on the time between injury and MRI. With grade 3 injuries, there is loss of continuity of ligamentous fibers (Fig. 15) and the ligament may have a wavy contour.

With chronic TCL tears, the ligament will appear thickened but its signal intensity will be normal and there will be no surrounding soft tissue edema. Calcification of the soft tissues adjacent to the femoral epicondyle (Pellegrini-Stieda disease) is best appreciated radiographically.

TCL bursitis is evident as high signal intensity between layers 2 (the superficial TCL) and 3 (the medial capsular ligament) [63]. A well-defined, elongated collection of fluid extending predominantly inferior to the joint may be observed without associated surrounding pathology.

Fibular collateral ligament

The fibular collateral ligament (FCL) is 5–7 cm long, extracapsular, and free from meniscal attachments. It courses from the lateral epicondyle of the femur posteriorly and inferiorly to the fibular head. It is crossed by the biceps tendon where an intervening bursa is present [64].

The FCL is best seen on posterior coronal images as a band of low signal intensity. Edema and hemorrhage, although less frequent than with TCL injury, may be seen with an acute, high-grade injury. With complete disruption of the FCL, a wavy contour and loss of ligamentous continuity may be evident (Fig. 16). While a normal appearance of the FCL is a reliable indication that the ligament is intact, nonvisualization does not imply pathology.

The posterolateral corner of the knee has a complex anatomy and contains several ligaments and tendons that contribute to rotatory stability. Some believe that the three most important static stabilizers are the fabellofibular ligament, the arcuate ligament, and the popliteal muscle including its tendon and origin. Others believe that the primary static stabilizer is the fibular origin of the popliteal muscle [65,66]. A hyperextension injury may result in external rotation and posterior subluxation of the lateral tibia with respect to the femur, an entity called posterolateral rotatory instability [67]. These injuries are not uncommon, and are difficult to detect clinically. MRI may be beneficial; however, work in this area is preliminary. MRI findings of injuries to the posterolateral ligaments include soft tissue edema adjacent to an intact but either thin or thick ligament, complete disruption, and increased intrasubstance T2 signal [68].

A major drawback in comparing the accuracy of MR findings with arthroscopy for injuries around the FCL and posterolateral corner of the knee is the extra-articular location of the fibular collateral, fabellofibular, arcuate, and popliteofibular ligaments [68]. In addition, the presence of the arcuate and fabellofibular ligaments has been shown to be inconsistent in cadaveric studies [69].

Coronal oblique imaging has been advocated to better depict the arcuate ligament and fibular origin of the popliteal muscle. Angling the coronal plane is thought to decrease volume averaging that could potentially obscure structures. Detection of the fabellofibular ligament seems to be dependent on positioning of the knee rather than an oblique imaging plane [69].

Meniscofemoral ligaments

The meniscofemoral ligaments consist of the ligament of Humphrey, which courses anterior to the PCL, and the ligament of Wrisberg, which courses posterior to the PCL (Fig. 17). Both originate on the posterior horn of

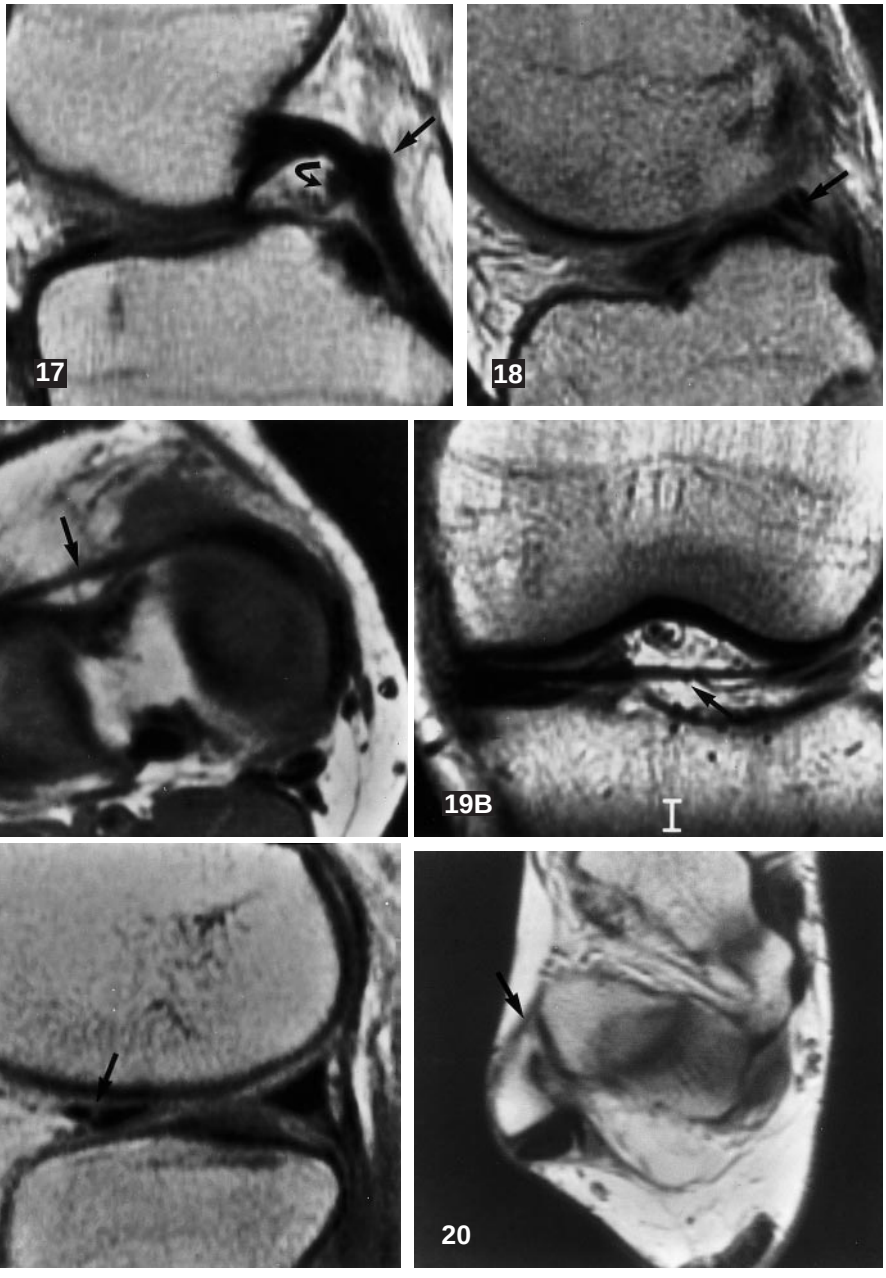

Fig. 17 Meniscofemoral ligaments of Humphry and Wrisberg. Sagittal T1-weighted MR image (SE 800/30) showing both ligaments (*curved arrow* Humphry, *straight arrow* Wrisberg)

Fig. 18 Pseudotear. Sagittal proton density MR image (SE 2200/20) showing a cleft (*arrow*) between the posterior horn of the lateral meniscus and the origin of the ligament of Humphry

Fig. 19A–C Normal transverse geniculate ligament. Axial T1-weighted MR image (**A**, SE 800/30) and coronal proton density MR image (**B**, SE 2200/30) showing the ligament (*arrow*) coursing between the anterior horns of the medial and lateral menisci. **C** A pseudotear (*arrow*) is present at the junction of the ligament and the anterior horn of the lateral meniscus (SE 2200/30)

Fig. 20 Normal anterior talofibular ligament. Axial oblique proton density MR image (SE 1800/20) showing the ligament as a thin low signal intensity band (*arrow*) coursing between the lateral malleolus and talus anteriorly

the lateral meniscus and insert on the medial wall of the intercondylar notch. A cleft between the meniscus and the ligament(s) at the origin may simulate a meniscal tear (Fig. 18). The meniscofemoral ligaments are considered to be stabilizers of the posterior horn of the lateral meniscus. The ligament of Humphrey is taut in flexion, and the ligament of Wrisberg is taut in extension.

The meniscofemoral ligaments may be appreciated in either coronal or sagittal images, but usually one ligament predominates. Either may be seen on approximately two-thirds of MR images (one-third each), but both are seen in only 3% of MR examinations [70].

Transverse geniculate ligament

The transverse geniculate ligament courses between the anterior horns of the medial and lateral meniscus, superficial to the joint capsule (Fig. 19A,B). As with the meniscofemoral ligaments, the interface between the ligament and the meniscus may simulate a tear (Fig. 19C). The ligament is of variable size, and is seen in over three-fourths of knee MR examinations [71].

Ankle and foot

Ankle sprains are common injuries, and most often involve the lateral ligaments. These include the anterior talofibular ligament (ATFL), the calcaneofibular ligament (CFL), and the posterior talofibular ligament (PTFL). Most injuries to the ankle result from inversion and internal rotation of the foot with ankle plantar flexion. Typically, these involve the ATFL since it is the weakest of the lateral ligaments [72].

The ATFL is the shortest of the three lateral ankle ligaments (Fig. 20). It courses from the anterior margin of lateral malleolus to insert on the talus [73]. Its primary function is to restrain internal rotation. The ATFL is best seen on axial or axial oblique images.

After the ATFL fails, the CFL is usually the next to tear [72]. The CFL is a cordlike structure that courses from the apex of lateral malleolus posteroinferiorly to the calcaneal tubercle [73] (Fig. 21). The ligament protects against varus forces. It is seen on MRI in the axial and coronal planes [74]. CFL tears can result in communication between the ankle joint and peroneal tendon sheaths [75].

The PTFL is the deepest lateral ligament. It extends from the inner posterior lateral malleolus to a prominent tubercle on the posterior surface of the talus [73] (Fig. 22). The posterior intermalleolar ligament may be seen superior to the PTFL on coronal images [76] (Fig. 22). While the PTFL rarely ruptures, PTFL injuries are almost always associated with ATFL and CFL tears [77].

The normal ankle ligaments are of low signal intensity; however, they may have longitudinal regions or striations of intermediate signal intensity [78,79]. An acute ligament tear is often evident as a focal disruption [78]. Ligament trauma may also be evident as increased intrasubstance signal, attenuation, waviness or tortuosity, or complete absence [79] (Fig. 23). In the acute to subacute setting, accompanying high signal may be present in the adjacent soft tissues or a joint effusion may be present [77].

Clinical grades of ankle injuries have been described, and are useful in determining prognosis with conservative treatment. A grade I injury is stretching or partial tear of ATFL. A grade II injury is complete tear of ATFL with other ligaments remaining intact. Grade III indicates complete tear of the ATFL and partial tear of the CFL, and grade IV is complete tear of both ligaments [80]. Typically, grade I and II injuries heal without significant instability. Grade III or IV injury have a higher predisposition to chronic pain that may eventually require surgical intervention [80].

Some authors argue that MRI is useful in the setting of an acute ankle injury, as clinical assessment is difficult in the presence of swelling and effusion and stress radiographs may not be possible without anesthesia. Most, however, feel that the vast majority of ankle sprains will heal, and MRI should be reserved for those individuals who do not respond to conservative treatment [81]. Importantly, it has been shown that MRI cannot reliably predict clinical outcome [82].

In the setting of chronic pain or instability following ankle injury, MRI may be useful for operative planning for ligament reconstruction. The sensitivity, specificity, and accuracy of MRI as compared with the operative findings have been shown to be 91.7–100%, 50–100%, and 94.4% respectively, depending on the ligament evaluated [83].

Anterolateral ankle impingement has received attention in the literature. This condition can result from a chronic ATFL tear, resulting in periligamentous hypertrophic synovitis, scarring, and fibrosis [84] (Fig. 24). This so-called meniscoid lesion can cause chronic ankle pain [85, 86]. The anteroinferior tibiofibular ligament can also cause anterolateral impingement when an inferior accessory fascicle is present [87]. Literature regarding the ability of MRI to depict anterolateral impingement is contradictory. While some authors feel that the diagnosis can be suggested by MRI [88], others have found MRI to be insensitive for this diagnosis [89].

The spring (plantar calcaneonavicular) ligament (Fig. 25) is visualized inconsistently on MRI due to its complex course [90]. This ligament, which extends from the anterior margin of the sustentaculum tali to the undersurface of the navicular, is a major stabilizing structure of the longitudinal arch of the foot [73]. Injury to the ligament may result in pes planovalgus, or flatfoot deformity [91].

The deltoid or medial collateral ligament is a strong triangular band that runs from the anterior and posterior borders of the medial malleolus to its insertion on the navicular and inferior spring ligament [73]. The ligament consists of the anterior and posterior tibiotalar, tibionavicular, and tibiocalcaneal ligaments [92]. The deltoid ligament rarely ruptures. If it does tear, there is often an associated avulsion fracture of medial malleolus [93]. Inflammatory or edematous changes without complete disruption may be seen on MRI. Focal areas of abnormal signal intensity are more commonly seen than complete absence of the ligament [93].

MR arthrography has been shown to be effective in detecting internal derangement of the lateral ankle ligaments. In one series, MR arthrography was 100% sensitive in diagnosing ATFL tears, and 90% sensitive in detecting CFL tears [94]. In this study, conventional MRI yielded a sensitivity of only 50% in detecting ATFL and CFL tears which, by the authors' own admission, is substantially less that that reported by others [95].

Shoulder

Glenohumeral instability can be an elusive clinical diagnosis. Either inherent laxity or injury to the labrocapsular

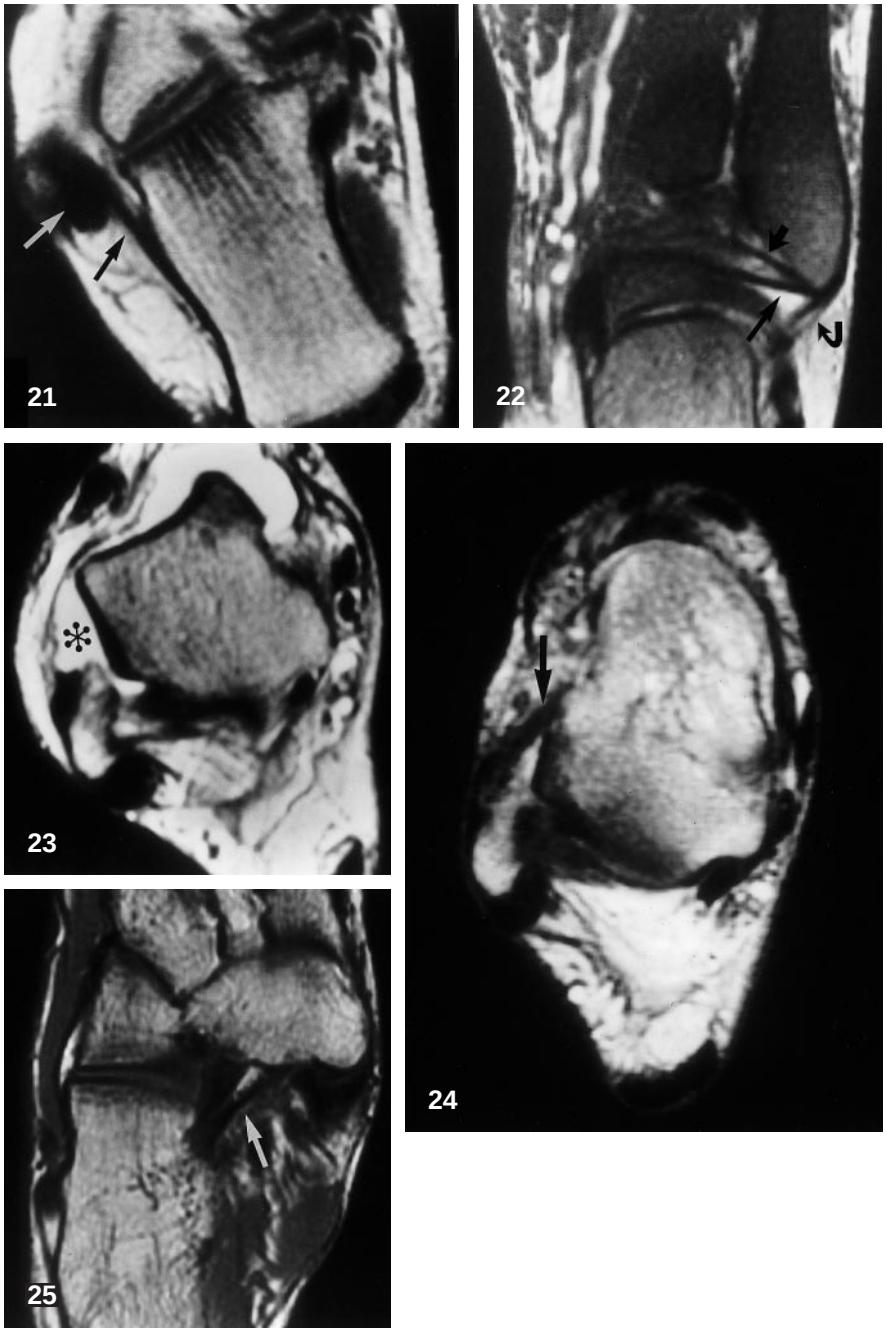

Fig. 21 Normal calcaneofibular ligament. Axial proton density MR image (SE 1800/30) showing the ligament (*black arrow*) coursing along the lateral aspect of the calcaneus, deep to the peroneal tendons (*white arrow*)

Fig. 22 Normal calcaneofibular, posterior talofibular, and posterior intermalleolar ligaments. Coronal proton density T2-FSE MR image (2766/70) showing the calcaneofibular (*curved arrow*), posterior talofibular (*straight arrow*), and posterior intermalleolar (*short arrow*) ligaments

Fig. 23 Torn anterior talofibular ligament following an acute inversion injury. Axial T2-weighted MR image (SE 1700/70) showing that the anterior talofibular ligament is absent, and the anterolateral gutter (*asterisk*) is filled with fluid from the large ankle effusion

Fig. 24 Anterolateral impingement. Axial proton density MR image (SE 1800/20) showing thickening of the anterior talofibular ligament (*arrow*) following a remote injury. Impingement was proven at arthroscopy

Fig. 25 Normal spring (plantar calcaneonavicular) ligament. Axial proton density MR image (SE 1800/20) showing the plantar fibers (*arrow*)

ligamentous complex (LCLC) may contribute to glenohumeral instability, a potentially debilitating problem of young, active individuals.

The LCLC consists of anterior and posterior parts. The anterior LCLC is comprised of the anterior joint capsule, labrum, glenoid fossa, anterior glenohumeral ligaments (superior, middle and inferior), and subscapular musculotendinous unit. The posterior portion consists of the posterior labrum, glenoid fossa, capsule, and posterior band of the IGL. The glenohumeral joint is one of the most mobile joints, and consequently has the least amount of intrinsic stability of any joint in the body.

The glenohumeral ligaments are focal thickenings of the joint capsule. Along with the coracohumeral ligament, they form a "Z" configuration [96]. The inferior glenohumeral ligament (IGL), is the largest and is formed by an anterior and posterior band. The axillary pouch intervenes between the two bands. The IGL has been implicated as a major stabilizer of the glenohumeral joint [97, 98]. The middle glenohumeral ligament (MGL) courses from the

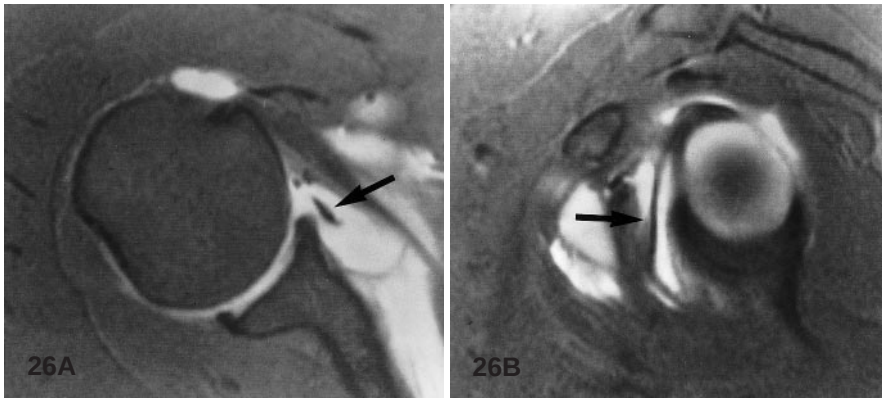

Fig. 26A,B Normal middle glenohumeral ligament. Axial (**A**) and sagittal oblique (**B**) fat-suppressed T1-weighted MR images (SE 583/15) after intra-articular gadolinium injection showing the middle glenohumeral ligament (*arrow*) as a thin band that extends between the anterosuperior glenoid and the lesser tuberosity of the humerus

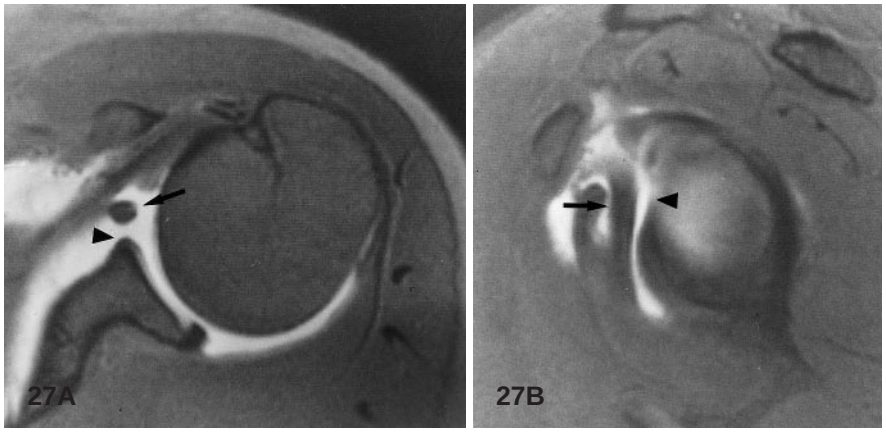

Fig. 27A,B Buford complex. Axial (**A**) and sagittal oblique (**B**) fat-suppressed T1-weighted MR images (SE 516/13) after intra-articular gadolinium injection. The middle glenohumeral ligament (*arrow*) is thick, and the anterior labrum (*arrowhead*) is absent. This normal variant should not be mistaken for a Bankart lesion

Fig. 28 Normal coracoacromial ligament. Sagittal oblique T2-FSE MR image (SE 2200/95) showing the ligament (*arrow*) as a thin, low signal intensity band running between the coracoid process and the anterior acromion

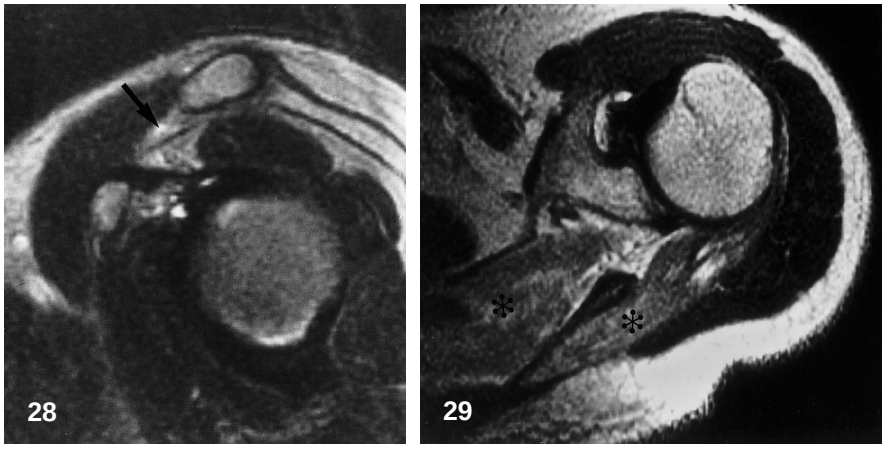

Fig. 29 Suprascapular nerve entrapment. Axial T2-weighted MR image (SE 1800/80) showing atrophy and/or edema of the supraspinatus and infraspinatus muscles (*asterisks*). This pattern is seen with abnormalities at the level of the notch including compression by the adjacent soft tissues or scapula, or stretching of the nerve itself. At surgery, the superior transverse scapular ligament was found to be thickened, apparently from a prior injury

anterosuperior glenoid to the lesser tuberosity (Fig. 26). This ligament may be injured by falling backwards on an outstretched arm or with weight lifting and bench pressing [96]. The MGL is less consistent than the IGL [96]. The superior glenohumeral ligament (SGL) originates from the superior glenoid fossa just anterior to the origin of the long head of the biceps tendon. It inserts on the lesser tuberosity where it blends with the coracohumeral ligament [96, 99]. The SGL, along with the coracohumeral ligament, restrains posterior and inferior translocation of the glenohumeral joint. It is often difficult to see on MRI [100].

The LCLC has been shown to have variable anatomy on conventional MRI in asymptomatic individuals [100, 101]. One normal variant to be aware of is the Buford complex [102] (Fig. 27). This is characterized by absence of the anterosuperior labrum and a "cordlike" MGL.

MR arthrography is useful for assessing the integrity of the LCLC [103–105]. The sensitivity and specificity of MR arthrography for the detection of labral and gle-

nohumeral ligamentous abnormalities compared with open or arthroscopic surgery have both been reported to be 88–100%, depending on which glenohumeral ligament was evaluated [105]. Another series reports the sensitivity and specificity of MR arthrography in the detection of labral abnormalities to be 91% and 93%, respectively [103].

Extra-articular ligaments of the shoulder girdle include the coracoacromial, coracohumeral, transverse humeral, and superior transverse scapular ligaments. The coracoacromial ligament is a key structure in the coracoacromial arch, and plays an important role in impingement [106] (Fig. 28). It is a strong triangular band that bridges the coracoid and acromial processes [107], and is consistently seen on sagittal oblique MR images. This ligament is usually resected at the time of acromioplasty for chronic impingement.

The coracohumeral ligament originates along the lateral aspect of the coracoid process, and blends with the transverse humeral ligament along the upper intertubercular sulcus. It assists in strengthening the joint capsule.

The transverse humeral ligament crosses the intertubercular sulcus, holding the long head of the biceps tendon within the groove. If disrupted, the long head of the biceps tendon may sublux medially.

The superior transverse scapular ligament traverses the suprascapular notch, the structure through which the suprascapular nerve passes before innervating the infraspinatus and supraspinatus muscles. While suprascapular nerve entrapment is most often due to compression on the nerve by a ganglion cyst, entrapment may also follow trauma where fracture fragments or scar tissue in the region of the ligament compress the nerve (Fig. 29).

Conclusion

Several large ligamentous structures are commonly investigated with routine MRI, but controversy exists as to the role of MRI in assessing some of the smaller ligaments of the body. As technological advances allow more detailed examination of these structures, our knowledge of normal anatomy, normal variants, and pathologic conditions will allow for more accurate and detailed examinations.

References

1. Gundry CR, Brahme SK, Schwaighofer B, Kang HS, Sartoris DJ, Resnick D. Is MR better than arthrography for evaluating the ligaments of the wrist? In vitro study. AJR 1990; 154:337–341.
2. Dalinka MK. MR imaging of the wrist. AJR 1995; 164:1–9.
3. Oneson SR, Timins ME, Scales LM, Erickson SJ, Chamoy L. MR imaging diagnosis of triangular fibrocartilage pathology with arthroscopic correlation. AJR 1997; 168:1513–1518.
4. Smith DK. Scapholunate interosseous ligament of the wrist: MR appearances in asymptomatic volunteers and arthrographically normal wrists. Radiology 1994; 192:217–221.
5. Totterman SMS, Miller RJ. Scapholunate ligament: normal MR appearance on three-dimensional gradient-recalled-echo images. Radiology 1996; 200:237–241.
6. Smith DK. Volar carpal ligaments of the wrist: normal appearance on multiplanar reconstructions of three-dimensional Fourier transform MR imaging. AJR 1993; 161:353–357.
7. Smith DK. Dorsal carpal ligaments of the wrist: normal appearance on multiplanar reconstructions of three-dimensional Fourier transform MR imaging. AJR 1993; 161:119–125.
8. Rominger MB, Bernreuter WK, Kenney PJ, Lee DH. MR imaging of anatomy and tears of wrist ligaments. Radiographics 1993; 13:1233–1246.
9. Timins ME, Jahnke JP, Krah SF, Erickson SJ, Carrera GF. MR imaging of the major carpal stabilizing ligaments: normal anatomy and clinical examples. Radiographics 1995; 15: 575–587.
10. Totterman SM, Heberger R, Miller R, et al. Two-piece wrist surface coil. AJR 1991; 156:343–344.
11. Wong EC, Jesmanowicz A, Hyde JS. High-resolution, short echo time MR imaging of the fingers and wrist with a local gradient coil. Radiology 1991; 181:393–397.
12. Schweitzer ME, Brahme SK, Hodler J, et al. Chronic wrist pain: spin-echo and short tau inversion recovery MR imaging and conventional and MR arthrography. Radiology 1992; 182:205–211.
13. Mikic ZD. Age changes in the triangular fibrocartilage of the wrist joint. J Anat 1978; 126:367–384.
14. Viegas SF, Ballantyne G. Attritional lesions of the wrist joint. J Hand Surg [Am] 1987; 12:1025–1029.
15. Metz VM, Schratter M, Dock WI, et al. Age-associated changes of the triangular fibrocartilage of the wrist: evaluation of the diagnostic performance of MR imaging. Radiology 1992; 184:217–220.
16. Manaster BJ, Mann RJ, Rubenstein S. Wrist pain: correlation of clinical and plain film findings with arthrographic results. J Hand Surg [Am] 1989; 14:466–473.
17. Metz VM, Mann FA, Gilula LA. Lack of correlation between site of wrist pain and location of noncommunicating defects shown by three-compartment wrist arthrography. AJR 1993; 160:1239–1243.
18. Campbell CS. Gamekeeper's thumb. J Bone Joint Surg Br 1955; 37:148–149.
19. Stener B. Displacement of the ruptured ulnar collateral ligament of the metacarpo-phalangeal joint of the thumb: a clinical and anatomical study. J Bone Joint Surg Br 1962; 44:869–879.
20. Bowers WH, Hurst LC. Gamekeeper's thumb: evaluation by arthrography and stress roentgenography. J Bone Joint Surg Am 1977; 59:519–524.
21. Campbell JD, Feagin JA, King P, Lambert KL, Cunningham R. Ulnar collateral ligament injury of the thumb: treatment with glove spica cast. Clinical notes. Am J Sports Med 1992; 20:29–30.
22. Spaeth HJ, Abrams RA, Bock GW, et al. Gamekeeper thumb: differentiation of nondisplaced and displaced tears of the ulnar collateral ligament with MR imaging. Work in progress. Radiology 1993; 188:553–556.

23. Hinke DH, Erickson SJ, Chamoy L, Timins ME. Ulnar collateral ligament of the thumb: MR findings in cadavers, volunteers, and patients with ligamentous injury (gamekeeper's thumb). AJR 1994; 163:1431–1434.
24. Harper MT, Chandnani VP, Spaeth J, Santangelo JR, Providence BC, Bagg MA. Gamekeeper thumb: diagnosis of ulnar collateral ligament injury using magnetic resonance imaging, magnetic resonance arthrography and stress radiography. J Magn Reson Imaging 1996; 6:322–328.
25. Ahn JM, Sartoris DJ, Kang HS, et al. Gamekeeper thumb: comparison of MR arthrography with conventional arthrography and MR imaging in cadavers. Radiology 1998; 206:737–744.
26. Ho CP. Sport and occupational injuries of the elbow: MR imaging findings [pictorial essay]. AJR 1995; 164:1465–1471.
27. Murphy BJ. MR imaging of the elbow. Radiology 1992; 184:525–529.
28. Sonin AH, Tutton SM, Fitzgerald SW, Peduto AJ. MR imaging of the adult elbow [scientific exhibit]. Radiographics 1996; 16:1323–1336.
29. Schwartz ML, Al-Zahrani S, Morwessel RM, Andrews JR. Ulnar collateral ligament injury in the throwing athlete: evaluation with saline-enhanced MR arthrography. Radiology 1995; 197:297–299.
30. Hergan K, Mittler C, Oser W. Ulnar collateral ligament: differentiation of displaced and nondisplaced tears with US and MR imaging. Radiology 1995; 194:65–71.
31. Anderson JE, ed. Grant's atlas of anatomy, 7th edn. Baltimore: Williams & Wilkins, 1978:fig. 6–57.
32. Jobe FW, Nuber G. Throwing injuries of the elbow. Clin Sports Med 1986; 5:621–636.
33. Cotten A, Jacobson J, Brossman J, et al. Collateral ligaments of the elbow: conventional MR imaging and MR arthrography with coronal oblique plane and elbow flexion. Radiology 1997; 204:806–812.
34. Sonin AH, Fitzgerald SW. MR imaging of sports injuries in the adult elbow: a tailored approach. AJR 1996; 167:325–331.
35. Glajchen N, Schwartz ML, Andrews JR, Gladstone J. Avulsion fracture of the sublime tubercle of the ulna: a newly recognized injury in the throwing athlete. AJR 1998; 170:627–628.
36. O'Driscoll SW, Bell DF, Morrey BF. Posterolateral rotatory instability of the elbow. J Bone Joint Surg Am 1991; 73:440–446.
37. Potter HG, Weiland AJ, Schatz JA, Paletta GA, Hotchkiss RN. Posterolateral rotatory instability of the elbow: usefulness of MR imaging in diagnosis. Radiology 1997; 204:185–189.
38. Timmerman LA, Andrews JR. Undersurface tear of the ulnar collateral ligament in baseball players: a newly recognized lesion. Am J Sports Med 1994; 22:33–36.
39. Girgis FG, Marshall JL, Al Monajem ARS. The cruciate ligaments of the knee joint: anatomical, functional and experimental analysis. Clin Orthop 1975; 106:216–231.
40. Tria AJ, Klein KS, eds. An illustrated guide to the knee. New York: Churchill Livingstone, 1992:86.
41. Maffulli N, Binfield PM, King JB, Good CJ. Acute haemarthrosis of the knee in athletes: a prospective study of 106 cases. J Bone Joint Surg Br 1993; 75:945–949.
42. Lee JK, Yao L, Phelps CT, Wirth CR, Czajka J, Lozman J. Anterior cruciate ligament tears: MR imaging compared with arthroscopy and clinical tests. Radiology 1988; 166:861–864.
43. Tung GA, Davis LM, Wiggins ME, Fadale PD. Tears of the anterior cruciate ligament: primary and secondary signs at MR imaging. Radiology 1993; 188:661–667.
44. Buckwalter KA, Pennes DR. Anterior cruciate ligament: oblique sagittal MR imaging. Radiology 1990; 175:276–277.
45. Gentili A, Seeger LL, Yao L, Do HM. Anterior cruciate ligament tear: indirect signs at MR imaging. Radiology 1994; 193:835–840.
46. Umans H, Wimpfheimer O, Haramati N, Applebaum YH, Adler M, Bosco J. Diagnosis of partial tears of the anterior cruciate ligament of the knee: value of MR imaging. AJR 1995; 165:893–897.
47. Yao L, Gentili A, Petrus L, Lee JK. Partial ACL rupture: an MR diagnosis? Skeletal Radiol 1995; 24:247–251.
48. Wasilewski SA, Frankl U. Osteochondral avulsion fracture of femoral insertion of anterior cruciate ligament: case report and review of literature. Am J Sports Med 1992; 20:224–226.
49. Rule JP, Seeger LL, Yao L, Shapiro S. Anterior cruciate ligament avulsion in active adults. Phys Sportsmed 1995; 23:25–32.
50. Schatz JA, Potter HG, Rodeo SA, Hannafin JA, Wickiewicz TL. MR imaging of anterior cruciate ligament reconstruction [pictorial essay]. AJR 1997; 169:223–228.
51. Howell SM, Knox KE, Farley TE, Taylor MA. Revascularization of the human anterior cruciate ligament graft during the first two years of implantation. Am J Sports Med 1995; 23:42–49.
52. Recht MP, Piraino DW, Applegate G, et al. Complications after anterior cruciate ligament reconstruction: radiographic and MR findings [pictorial essay]. AJR 1996; 167:705–710.
53. Mueller W. The knee: form, function and ligament reconstruction. Berlin Heidelberg New York: Springer, 1983:214–216.
54. Kennedy JC, Hawkins RJ, Willis RB, Danylchuk KD. Tension studies of human knee ligaments. J Bone Joint Surg Am 1976; 58:350–355.
55. Grover JS, Bassett LW, Gross ML, Seeger LL, Finerman GAM. Posterior cruciate ligament: MR imaging. Radiology 1990; 174:527–530.
56. Sonin AH, Fitzgerald SW, Friedman H, Hoff FL, Hendrix RW, Rogers LF. Posterior cruciate ligament injury: MR imaging diagnosis and patterns of injury. Radiology 1994; 190:455–458.
57. Sonin AH, Fitzgerald SW, Hoff FL, Friedman H, Bresler ME. MR imaging of the posterior cruciate ligament: normal, abnormal, and associated injury patterns. Radiographics 1995; 15:551–561.
58. Warren LF, Marshall JL. The supporting structures and layers on the medial side of the knee. J Bone Joint Surg Am 1979; 61:56–62.
59. Fetto JF, Marshall JL. Medial collateral ligament injuries of the knee: a rationale for treatment. Clin Orthop 1978; 132:206–218.
60. Shelbourne KD, Nitz PA. The O'Donoghue triad revisited: combined knee injuries involving anterior cruciate and medial collateral ligament tears. Am J Sports Med 1991; 19:474–477.
61. Duncan JB, Hunter R, Purnell M, Freeman J. Meniscal injuries associated with acute anterior cruciate ligament tears in alpine skiers. Am J Sports Med 1995; 23:170–172.
62. Schweitzer ME, Tran D, Deely DM, Hume EL. Medial collateral ligament injuries: evaluation of multiple signs, prevalence and location of associated bone bruises, and assessment with MR imaging. Radiology 1995; 194:825–829.
63. Lee JK, Yao L. Tibial collateral ligament bursa: MR imaging. Radiology 1991; 178:855–857.
64. Pick TP, Howden R. Gray's Anatomy: anatomy, descriptive and surgical, 15th edn. New York: Bounty Books, 1977:274–276.
65. Sudasna S, Harnsiriwattanagit K. The ligamentous structures of the posterolateral aspect of the knee. Bull Hosp Jt Dis Orthop Inst 1990; 50:35–40.

66. Watanabe Y, Moriya H, Takahashi K, et al. Functional anatomy of the posterolateral structures of the knee. Arthroscopy 1993; 9:57–62.
67. Hughston JC, Jacobson KE. Chronic posterolateral rotatory instability of the knee. J Bone Joint Surg Am 1985; 67:351–359.
68. Miller TT, Gladden P, Staron RB, Henry JH, Feldman F. Posterolateral stabilizers of the knee: anatomy and injuries assessed with MR imaging. AJR 1997; 169:1641–1647.
69. Yu JS, Salonen DC, Hodler J, et al. Posterolateral aspect of the knee: improved MR imaging with a coronal oblique technique. Radiology 1996; 198:199–204.
70. Watanabe AT, Carter BC, Teitelbaum GP, Bradley WG Jr. Common pitfalls in magnetic resonance imaging of the knee. J Bone Joint Surg Am 1989; 71:857–862.
71. Sintzoff SA Jr, Gevenois PA, Andrianne Y, Struyven J. Transverse geniculate ligament of the knee: appearance at plain radiography. Radiology 1991; 180:259.
72. Marder RA. Current methods for the evaluation of ankle ligaments injuries: an instructional course lecture. J Bone Joint Surg Am 1994; 76:1103–1111.
73. Pick TP, Howden R. Gray's anatomy: anatomy, descriptive and surgical, 15th edn. New York: Bounty Books, 1977:283–288.
74. Schneck CD, Mesgarzadeh M, Bonakdarpour A, Ross GJ. MR imaging of the most commonly injured ankle ligaments. 1. Normal anatomy. Radiology 1992; 184:499–506.
75. Raatikainen T, Putkonen M, Puranen J. Arthrography, clinical examination, and stress radiograph in the diagnosis of acute injury to the lateral ligaments of the ankle. Am J Sports Med 1992; 20:2–6.
76. Erickson SJ, Smith JW, Ruiz ME, et al. MR imaging of the lateral collateral ligament of the ankle [pictorial essay]. AJR 1991; 156:131–136.
77. Rosenberg ZS, Cheung YY, Beltran J, Sheskier S, Leong M, Jahaa M. Posterior intermalleolar ligament of the ankle: normal anatomy and MR imaging features. AJR 1995; 165:387–390.
78. Kier R, McCarthy S, Dietz MJ, Rudicel S. MR appearance of painful conditions of the ankle. Radiographics 1991; 11:401–414.
79. Link SC, Erickson SJ, Timins ME. MR imaging of the ankle and foot: normal structures and anatomic variants that may simulate disease [pictorial essay]. AJR 1993; 161:607–612.
80. Rijke AM, Goitz HT, McCue FC, Dee PM. Magnetic resonance imaging of injury to the lateral ankle ligaments. Am J Sports Med 1993; 21:528–534.
81. Boruta PM, Bishop JO, Braly WG, Tullos HS. Acute lateral ankle ligament injuries: a literature review. Foot Ankle 1990; 11:107–113.
82. Zanetti M, DeSimoni D, Wetz HH, Zollinger H, Hodler J. Magnetic resonance imaging of injuries of the ankle joint: can it predict clinical outcome? Skeletal Radiol 1997; 26:82–88.
83. Verhaven EF, Shahabpour M, Handelberg FW, Vaes PH, Opdecam PH. The accuracy of three-dimensional magnetic resonance imaging in the diagnosis of ruptures of the lateral ligaments of the ankle. Am J Sports Med 1991; 19:583–587.
84. Ferkel RD, Karzel RP, Del Pizzo W, Friedman MJ, Fischer SP. Arthroscopic treatment of anterolateral impingement of the ankle. Am J Sports Med 1991; 19:440–446.
85. Wolin I, Glassman F, Sideman S, Levinthal DH. Internal derangement of the talofibular component of the ankle. Surg Gynecol Obstet 1950; 91:193–200.
86. Stone JW, Guhl JF. Meniscoid lesions of the ankle. Clin Sport Med 1991; 10:661–676.
87. Bassett FH III, Gates HS III, Billys JB, Morris HB, Nikolaou PK. Talar impingement by the anteroinferior tibiofibular ligament. J Bone Joint Surg Am 1990; 72:55–59.
88. Rubin DA, Tishkoff NW, Britton CA, Conti SF, Towers JD. Anterolateral soft-tissue impingement in the ankle: diagnosis using MR imaging. AJR 1997; 169:829–835.
89. Farooki S, Yao L, Seeger LL. Anterolateral impingement of the ankle: effectiveness of MR imaging. Radiology 1998; 207:357–360.
90. Rule J, Yao L, Seeger LL. Spring ligament of the ankle: normal MR anatomy [pictorial essay]. AJR 1993; 161:1241–1244.
91. Borton DC, Saxby TS. Tear of the plantar calcaneonavicular (spring) ligament causing flatfoot: a case report. J Bone Joint Surg Br 1997; 79:641–643.
92. Netter FH. Atlas of human anatomy. Summit, NJ: Ciba-Geigy, 1989: plate 495.
93. Klein MA. MR imaging of the ankle: normal and abnormal findings in the medial collateral ligament [pictorial essay]. AJR 1994; 162:377–383.
94. Chandnani VP, Harper MT, Ficke JR, et al. Chronic ankle instability: evaluation with MR arthrography, MR imaging, and stress radiography. Radiology 1994; 192:189–194.
95. Verhaven EFC, Shahabpour M, Handleberg FWJ, Vaes PHEG, Opdecam PJE. The accuracy of three-dimensional magnetic resonance imaging in the diagnosis of ruptures of the lateral ligaments of the ankle. Am J Sports Med 1991; 19:583–587.
96. Ferrari DA. Capsular ligaments of the shoulder: anatomical and functional study of the anterior superior capsule. Am J Sports Med 1990; 18:20–24.
97. Moseley HF, Övergaard B. The anterior capsular mechanism in recurrent anterior dislocation of the shoulder: morphological and clinical studies with special reference to the glenoid labrum and the gleno-humeral ligaments. J Bone Joint Surg Br 1962; 44:913–927.
98. Turkel SJ, Panio MW, Marshall JL, Girgis FG. Stabilizing mechanisms preventing anterior dislocation of the glenohumeral joint. J Bone Joint Surg Am 1981; 63:1208–1217.
99. Coumas JM, Waite RJ, Goss TP, Ferrari DA, Kanzaria PK, Pappas AM. CT and MR evaluation of the labral capsular ligamentous complex of the shoulder. AJR 1992; 158:591–597.
100. Liou JTS, Wilson AJ, Totty WG, Brown JJ. The normal shoulder: common variations that simulate pathologic conditions at MR imaging. Radiology 1993; 186: 435–441.
101. Neumann CH, Petersen SA, Jahnke AH. MR imaging of the labral-capsular complex: normal variations. AJR 1991; 157:1015–1021.
102. Tirman PFJ, Feller JF, Palmer WE, Carroll KW, Steinbach LS, Cox I. The Buford complex: a variation of the normal shoulder anatomy. MR arthrographic imaging features. AJR 1996; 166:869–873.
103. Palmer WE, Brown JH, Rosenthal DI. Labral-ligamentous complex of the shoulder: evaluation with MR arthrography. Radiology 1994; 190:645–651.
104. Massengill AD, Seeger LL, Yao L, et al. Labrocapsular ligamentous complex of the shoulder: normal anatomy, anatomic variation, and pitfalls of MR imaging and MR arthrography. Radiographics 1994; 14:1211–1223.
105. Chandnani VP, Gagliardi JA, Murnane TG, et al. Glenohumeral ligaments and shoulder capsular mechanism: evaluation with MR arthrography. Radiology 1995; 196:27–32.
106. Kessel L, Watson M. The painful arc syndrome: clinical classification as a guide to management. J Bone Joint Surg Br 1977; 59:166–172.
107. Pick TP, Howden R. Gray's anatomy: anatomy, descriptive and surgical, 15th edn. New York: Bounty Books, 1977:249–250.